EFDA–JET–CP(14)01/24

S. Potzel, M. Wischmeier, M. Bernert, R. Dux, F. Reimold, A. Scarabosio,
S. Brezinsek, M. Clever, A. Huber, A. Meigs, M. Stamp,
the ASDEX Upgrade Team and JET EFDA contributors

O-35 Formation of the High Density Front in the Inner Far SOL at ASDEX Upgrade and JET

O-35 Formation of the High Density Front in the Inner Far SOL at ASDEX Upgrade and JET

S. Potzel[1], M. Wischmeier[1], M. Bernert[1], R. Dux[1], F. Reimold[1], A. Scarabosio[1], S. Brezinsek[2], M. Clever[2], A. Huber[2], A. Meigs, M. Stamp, the ASDEX Upgrade Team[1] and JET EFDA contributors*

JET-EFDA, Culham Science Centre, OX14 3DB, Abingdon, UK

[1]Max-Planck-Institut für Plasmaphysik, Boltzmannstraße 2, 85748 Garching, Germany.
[2]Institute for Energy and Climate Research, Forschungszentrum Jülich GmbH, Jülich, Germany.
** See annex of F. Romanelli et al, "Overview of JET Results", (24th IAEA Fusion Energy Conference, San Diego, USA (2012)).*

Preprint of Paper to be submitted for publication in Proceedings of the
21st International Conference on Plasma Surface Interactions, Kanazawa, Japan
26th May 2014 – 30th May 2014

ABSTRACT

This article presents the development of a region of high electron density, being one order of magnitude larger than the separatrix density, in the inner divertor well above the X-point in ASDEX Upgrade and JET H-mode discharges. In order for this high-field side high density (HFSHD) to be formed, the inner divertor has to be detached while the outer one remains attached and the heating power has to be sufficiently high. The HFSHD, which is determined independently from spectroscopic and interferometric measurements, is clearly correlated with neutral fluxes in the far scrape-off layer; both increase with heating power. Injection of N_2 into the divertor private flux region leads to a suppression of the HFSHD in ASDEX Upgrade and JET. The density distribution in the inner divertor volume with and without N_2 seeding is consistent with the total radiation and the D_γ distribution.

1. INTRODUCTION

A major challenge of large future devices like ITER or DEMO is the power and particle exhaust in order to stay below the tolerable power load of the plasma facing components, which is currently estimated to be $5-10 MW/m^2$ given present PFC technology. Therefore, the divertor has to be operated in the highly radiative, partially detached regime [1]. In order to reach this regime in present day metallic devices, seeding of impurities such as Nitrogen is required in addition to a high Deuterium fuelling (e.g. [2]). Understanding and predicting divertor detachment is mandatory for future large scale devices.

Former L-mode studies in ASDEX Upgrade (AUG), equipped with a full W wall, revealed that during the fluctuating detachment state, where the inner divertor is already partially detached at the near separatrix region, while the outer is still attached, a region of high electron density forms in the inner far Scrape-off Layer (SOL) [3]. Injecting N_2 into the divertor plasma leads to a reduction of this high-field side high density (HFSHD) front [4]. In AUG H-mode discharges with a full carbon wall, high electron densities where observed at the entrance of the inner divertor in the HFS far SOL [5]. A quantitative interpretation of these effects, even with the most sophisticated codes, is not yet possible [6]. More experimental observations are needed to understand the physics and constrain the models.

Here we report on comparable observations in ASDEX Upgrade, equipped with a full W wall, and JET H-mode discharges, equipped with the ITER-Like wall (Be/W), showing that this effect is independent of confinement mode and machine size. The spatial extend of the HFSHD is much larger compared to L-mode and expands well above the X-point into the HFS main chamber. It will be further shown that injecting N_2 into the divertor of AUG and JET leads to a reduction or even suppression of the HFSHD, depending on the amount of injected N_2. It should be noted here that in metallic machines without intrinsic radiator N seeding acts like the intrinsic C radiator in carbon machines [7, 8]

2. THE HIGH DENSITY FRONT IN THE INNER SOL OF ASDEX UPGRADE

2.1. DIAGNOSTIC SETUP

The main diagnostics used to investigate the divertor plasma in the inner SOL of AUG are shown in figure 1. A vertical CO_2 interferometer (VIF) measures the line integrated electron density. Knowing the density profile of the confined plasma from other diagnostics, one can subtract this part from the interferometer measurement. This yields the line integrated density in the lower inner divertor SOL, assuming that the contribution from the upper divertor SOL can be neglected [5]. Another independent measure of the local n_e is by Stark broadening analysis (SBD) of the Balmer $D_\in$ line [9]. While the spectroscopic system covers the entire lower divertor, it is focused here only on two lines of sight (LOS) viewing vertically through the X-point and two LOS viewing at the upper part of the HFS SOL. The latter two LOS intersect also the outer divertor, but the $D_\in$ emission in this region is (except in cases with a strongly detached outer divertor) more than one order of magnitude lower than the emission in the inner divertor. Neutral fluxes are measured with AUG pressure gauges [11]. One of them is situated behind the the inner heat-shield at the entrance to the inner divertor and one below the divertor dome. The latter represents more the global recycling in the divertor while the former is is a measure of the local recycling in that upper part of the inner divertor, which results either from neutral leakage of the divertor or coming from the HFS main chamber due to poloidal SOL flows.

2.2. FORMATION OF THE HFSHD FRONT

Here, several H-mode discharges have been analyzed at AUG where the inner divertor plasma is partially detached at the vertical target component (flat ion saturation current profile and target temperatures below 5eV) whereas the outer divertor plasma remains attached. Time traces of a typical discharge are shown in figure 2. After reaching the current flat-top of 0.8MA and the desired line averaged density of $6.4 \times 10^{19}\mathrm{m}^{-3}$ at a toroidal magnetic field of 2.5 T, the gas fueling, applied from the main chamber outer mid-plane, is kept constant at a rate of 2×10^{22}el/s, resulting in a constant plasma density. Then the neutral beam heating is increased stepwise from 2.5 to 7.5MW and a maximum ECRH power of 1.6MW is applied to avoid impurity accumulation in the plasma center. Correlated with the increase of the heating power a high electron density develops in the HFS far SOL, measured with both, the SBD and the VIF interferometer (Figure 2c). The intersection length of the interferometer cord in the HFS SOL is approximately 10 cm, which yields an average electron density of $\approx 4.7 \times 10^{20}\mathrm{m}^{-3}$ during the highest heating phase. This density is similar to the one measured with the upper SBDH1 LOS (see Figure 1) and is ≈ 15% lower than the density measured with the SBDH2 LOS. This means that the HFSHD front decreases upwards but expands up to the entrance of the inner divertor well above the X-point. The electron density at the X-point of $\approx 2.7 \times 10^{20}\mathrm{m}^{-3}$ (measured with the SBDV LOS) is during the highest heating phase ≈ 40% lower than in the HFS far SOL. Also the neutral fluxes in the HFS far SOL, $\Gamma_{n,HFS}$, increase with increasing heating power, but the neutral fluxes in the PFR, $\Gamma_{n,PFR}$, as well as the line integrated

plasma density remain constant (Figure 2b,d). This means that the recycling in the HFS far SOL increases in combination with a decrease of the neutral compression ratio in the inner divertor. We define here the inner divertor neutral compression ratio as $\eta_{HFS} = \Gamma_{n,PFR}/\Gamma_{n,HFS}$, which drops significantly with increasing heating power (Figure 2d).

The same qualitative trend of the HFSHD front formation is observed in all discharges analyzed here, but its absolute values depend on the specific discharge parameters. Figure 3a shows the increase of the HFSHD measured with SBD and VIF with the heating power for all analyzed discharges. The scatter in the density at constant heating power is due to the fact that the main plasma density varies in the various discharges. In addition, geometric effects like the variation of the inner strike point position influences the density measurements. There is, however, a much clearer dependence of the HFSHD on $\Gamma_{n,HFS}$ and on η_{HFS} (Fig 3b,c). Whether the increasing heating power leads to the divertor neutral leakage and this causes the HFSHD, or the increased heating power increases the recycling in the far SOL, causing the HFSHD, is not clear yet. It must be noted here again that in all cases analyzed here, the inner divertor was detached at the vertical target component and increasing heating power did not cause a re-attachment. Moreover, the ion flux at the vertical inner target is more than one order of magnitude lower than the peak ion flux in the outer divertor and remains almost constant during the different heating steps.

2.3. REDUCTION OF HFSHD WITH N2 SEEDING

In AUG, Nitrogen is routinely injected in to cool the divertor [10]. The temperature reduction is caused by removing power in the SOL via line radiation. In the reference discharge discussed above, a constant Nitrogen injection of $\Gamma_N = 2.3 \times 10^{22}$ el/s was applied at $t = 2.8$s (Figure 2b). This leads to a strong reduction of both, the HFSHD front as well as the neutral fluxes in the inner far SOL (Figure 2c,d). The line integrated density and $\Gamma_{n,PFR}$ remain unaffected by the N_2 injection, while the inner divertor neutral compression ratio improves again (Figure 2b,d). This proves that the formation of the HFSHD and the increase of the neutral fluxes in the inner far SOL are connected to the power in the SOL. In addition, the electron density at the X-point, measured with the SBDV LOSs, increases with Nitrogen injection. The reconstructed total radiation in the divertor, shown in figure 4, is consistent with the other measurements. Without Nitrogen injection, there is a strong radiation in the HFS far SOL. Integrating the radiated power of discharge # 24681 in the HFS SOL from the X-point up to the HFS mid-plane yields a total radiated power in this region of $P_{rad,HFS} =$ 0.6MW, which is ≈ 10% of the total heating power. With Nitrogen injection the total radiation is reduced in the far SOL and peaks at the X-point. The peaking of the radiation and density at the X-point with Nitrogen injection is also observed in H-mode detachment experiments [2].

3. THE HIGH DENSITY FRONT AT JET

A high electron density front develops in the HFS far SOL during high density, high power H-mode discharges at JET, similar to the observations made at AUG. The H-mode discharges analyzed

at JET had a plasma current of 2.5MA, a toroidal magnetic field of 2.6T, a medium triangularity and a NBI power of 19MW. A deuterium fueling of 13.6×10^{22} el/s was applied, leading to a line integrated core density of $n_e \, dl = 1.8 \times 10^{20} m^{-2}$. No power scans have been done in this scenario so far, but different N_2 injection rates have been applied.

The electron density in the JET HFS SOL was determined with Stark broadening analysis of the Balmer D_δ line. Similar to AUG, synthetic Stark profiles [12], based on the Model Microfield method [12], are convoluted with the instrument function and the Doppler broadening of a fixed neutral temperature of T_n = 5eV and fitted to the measured line in a least square sens. The instrument function is obtained by a Gaussian fit to a neighboring Beryllium line, assuming the Doppler broadening of T_n = 5eV being the only additional broadening mechanism. An example fit is shown in Figure 5. The resulting densities are similar to the JET standard technique for the outer divertor [13] The spectroscopic system KSRD measuring the D_δ line in the HFS SOL consists of 10 vertically viewing LOS, which are shown in Figure 6b. The density profile in the HFS SOL is shown in Figure 7a, different symbols and colors refer to the corresponding LOS in Figure 6. From this LOS geometry it is clear that there is a high electron density of $\approx 2.8 \times 10^{20} m^{-3}$ in the HFS far SOL above the X-point (blue diamonds), which is almost as high as the density at the strike point region ($\approx 3.1 \times 10^{20} m^{-3}$, cyan LOS).

Figures 7b and c show the density profiles for similar discharges with an additional medium N_2 injection ($\Gamma_{N_2} = 6.4 \times 10^{22}$el/s, $n_e dl = 1.8 \times 10^{20} m^{-2}$, P_{NBI} = 18MW) and high N_2 injection ($\Gamma_{N_2} = 13.6 \times 10^{22}$ el/s, $n_e dl = 1.9 \times 10^{20} m^{-2}$, P_{NBI} = 18MW), respectively. In agreement with the AUG results, injection of N_2 leads to a reduction of the HFSHD front. In the medium N_2 injection case, only the density in the HFS far SOL is reduced but the profile still peaks at the strike point region (cyan LOS). With high N_2 injection the HFSHD front is suppressed and the density peaks now at the X-point, similar to AUG.

Moreover, the measured density distribution in the HFS SOL is consistent with both, the reconstructed total radiation and the D_γ distribution [14] in the divertor. Without N_2 injection there is a broad distribution of the total radiation in the HFS divertor volume and also in the far SOL well above the X-point, shown in Figure 8. In the case of the strong N_2 injection the total radiation peaks at the X-point and is reduced in the HFS far SOL. This observation is again in qualitative agreement with the AUG results. Figure 9a shows the D_γ distribution for the non N_2 injection case. Here, the D_γ emission in the HFS is very localized in front of the target. With strong N_2 injection, however, the D_γ emission is broadly distributed in the HFS SOL, even above the X-point (Figure 9b). This is consistent with the observations above, as D_γ radiates efficiently at low temperatures and is to some extend a measure for volume recombination [3]. Without N_2 injection the inner divertor plasma is hot due to the absence of an intrinsic impurity radiator [8], except in a thin region in front of the target (the inner divertor is already detached without N_2 injection). Injection of Nitrogen reduces the temperature in a large region of the HFS SOL, leading to a broad distribution of the D_γ emission.

4. DISCUSSION

From the experimental observations presented above it is evident that the formation of a high density, which is one order of magnitude larger than the separatrix density and located in the HFS far SOL above the X-point, is correlated with the power in the SOL. Whether the density in the far SOL results only due to recycling in that region or an additional enhanced radial transport is needed is not yet clear. Models proposing such an enhanced radial transport like shock-fronts require a strong parallel temperature gradient ([15]). The experimental observations are at least consistent with such a model. At all heating powers (shown in Figure 3a), the inner divertor remains detached and the temperature in front of the target is $\leq$ 5eV. Increasing the heating power would then lead to an increase of the power in the SOL which might shrink the region of the temperature gradient, i.e. steepening the gradient. Nitrogen radiates most sufficient at temperatures $10 \approx 30$eV, i.e. in regions above the cold target zone. N_2 injection thus might flatten the parallel temperature gradient again. A critical question validating this model is over which parallel length the temperature is reduced. The answer, however, can not be given based on the data presented here. The role of lowZ impurities might also be of importance here. In JET with the ITER-like wall the upper part of the inner divertor is covered with Beryllium. Local sputtering might enhance the density built-up in that region as Be is preferentially ionized in the SOL. AUG is completely covered with Tungsten, which mainly ionizes in the main plasma. However, there is Boron and still some residual Carbon in the machine and it is known that the inner divertor is an area of net deposition [16], leading to the formation of surface layers. B and C would then be sputtered and partly be ionized in that region and influence the local recycling. A quantitative investigation of this effect has still to be done.

5. SUMMARY AND OUTLOOK

The formation of a high density, which is one order of magnitude larger than the separatrix density and situated in the HFS far SOL well above the X-point, has been observed in AUG and JET H-mode discharges. The spatial extend into the far SOL is much larger in H-mode compared to previous findings in L-mode [3]. To trigger the HFSHD the inner divertor has to be detached and the heating power has to be sufficiently high. Moreover, applying more heating power increases the HFSHD while the main plasma density remains almost unchanged. Injection of N_2 at AUG and JET, hence radiating power in the SOL, reduces or suppresses the HFSHD front, depending on the amount of injected N_2 .

Detailed power-scans at AUG showed that both, the high density and the neutral fluxes in the HFS far SOL increase about linearly with heating power, whereas the neutral fluxes in the PFR and the line integrated plasma density remain unchanged. This means that there is also a clear correlation between the high density in the HFS far SOL and the neutral leakage in the inner divertor, which also increases with heating power. Further studies in both machines are required to understand these mechanisms.

6. ACKNOWLEDGMENTS

This project has received funding from the EURATOM research and training programme 2014–2018. This work was supported by EURATOM and carried out within the framework of the European Fusion Development Agreement. The views and opinions expressed herein do not necessarily reflect those of the European Commission.

REFERENCES

[1]. R.A. Pitts, et al., Journal of Nuclear Materials, **438** (2013) 48.
[2]. F. Reimold, et al., This conference.
[3]. S. Potzel, et al., Nuclear Fusion **54** (2014) 013001.
[4]. S. Potzel, et al., Journal of Nuclear Materials **438** (2013) S523.
[5]. K. McCormick, et al., Journal of Nuclear Materials **390–391** (2009) S465.
[6]. M. Wischmeier, et al., This conference.
[7]. R. Neu, et al., Physica Scripta **T138** (2009) 014038.
[8]. S. Brezinsek, et al., Journal of Nuclear Materials **438** (2013) S303.
[9]. S. Potzel, et al., Plasma Physics and Controlled Fusion **56** (2014) 025010
[10]. A. Kallenbach, et al., Plasma Physics and Controlled Fusion **52** (2010) 055002
[11]. A. Scarabosio, et al., Journal of Nuclear Materials **390–391** (2009) S494.
[12]. C. Stehl´e, et al., Astronomy and Astrophysics Supplement Series **140** (1999) 93.
[13]. A. Meigs, et al., Journal of Nuclear Materials **438** (2013) S607.
[14]. A. Huber, et al., Review of Scientific Instruments **83** (2012) 10D511
[15]. M. Wischmeier, et al., APS Conference 2014, Denver
[16]. A. Hakkola, et al., EPS Conference 2013, Helsinki, Finland

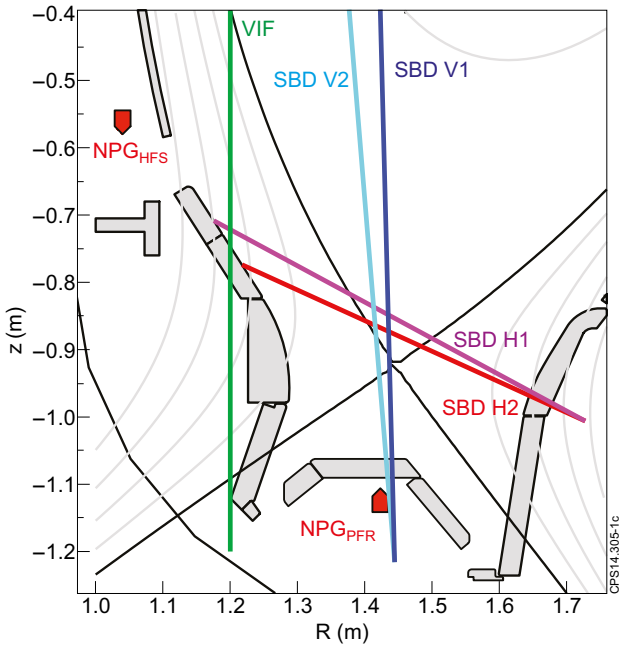

Figure 1: Main diagnostics used at AUG: CO_2 interferometer VIF (green), Stark broadening lines of sight SBDH1&2 (red & magenta), SBDV1&2 (dark & light blue) and neutral pressure gauges (red).

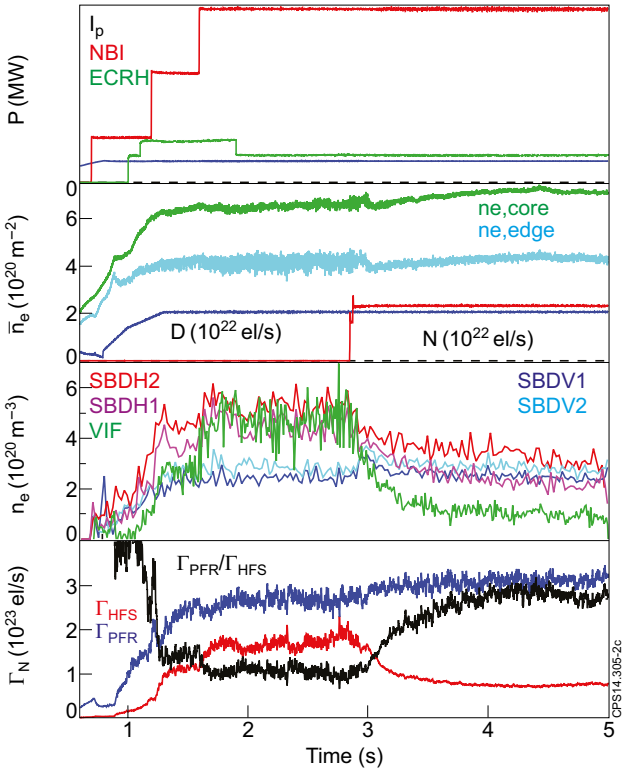

Figure 2: Time traces of AUG discharge # 29172 showing HFSHD front formation: (a) plasma current (blue), NBI (red) and ECRH (green) heating power; (b) line integrated core (green) and edge (cyan) density, Deuterium fueling (blue) and Nitrogen injection rate (red); (c) Density in the HFS far SOL measured with the SBDH LOS (red) and VIF (green) and at the X-point measured with the SBDV (blue) LOS; (d) the neutral fluxes in the PFR (blue) and HFS far SOL (red) and the inner divertor neutral compression ratio (black).

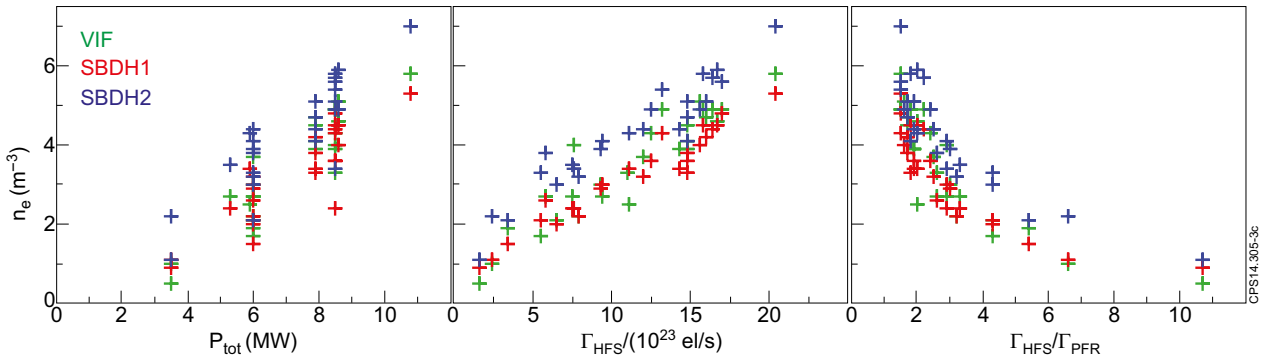

Figure 3: Density in the AUG HFS far SOL measured with VIF (green) and the SBDH1 (red) and SBDH2 (blue) LOS versus the total applied heating power (a), versus the neutral fluxes in the inner far SOL (b) and versus the inner divertor neutral compression ratio (c).

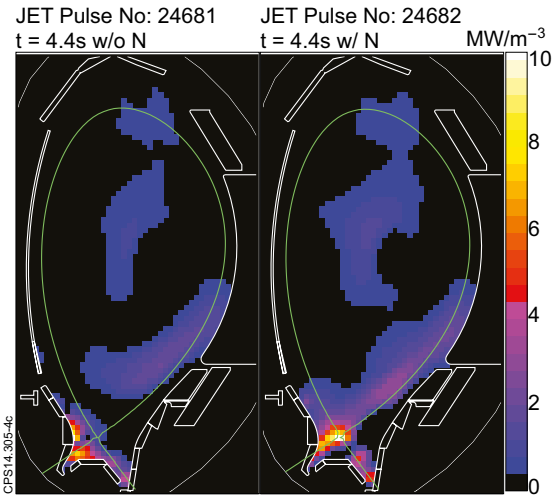

Figure 4: Reconstructed total radiance in the AUG divertor during HFSHD front formation without (a) N_2 injection and with (b) N_2 injection.

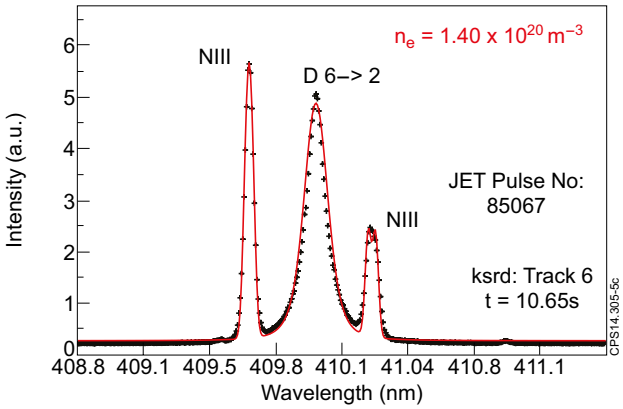

Figure 5: Example Stark fit on the Balmer D_δ line yielding the electron density. The two NII lines are fitted with a Gaussian only.

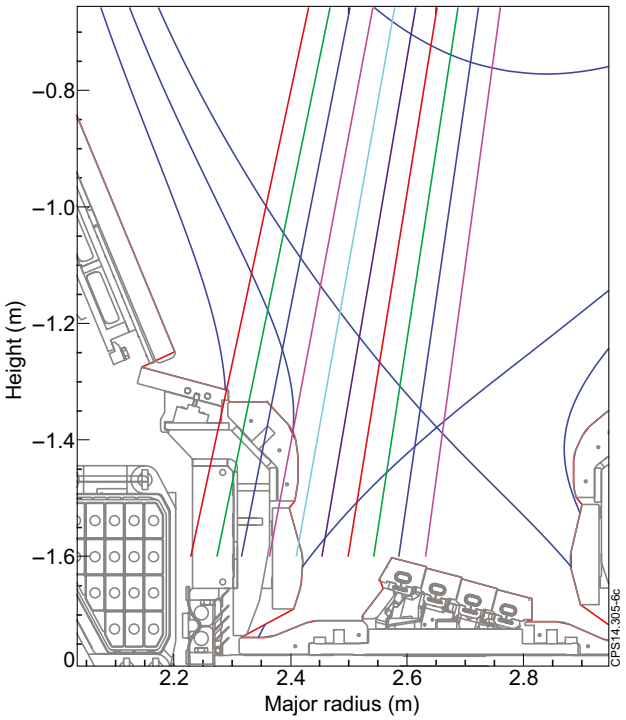

Figure 6: Geometry of the KSRD LOS measuring the D_δ line in the JET HFS SOL.

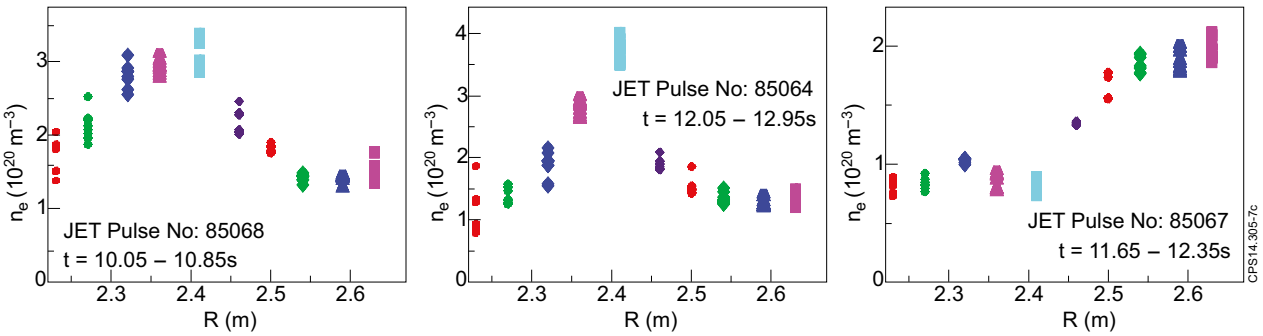

Figure 7: Electron density in HFS SOL measured with KSRD without (a), with medium (b) and high (c) N_2 injection. The color-code refer to the LOS shown in Figure 6.

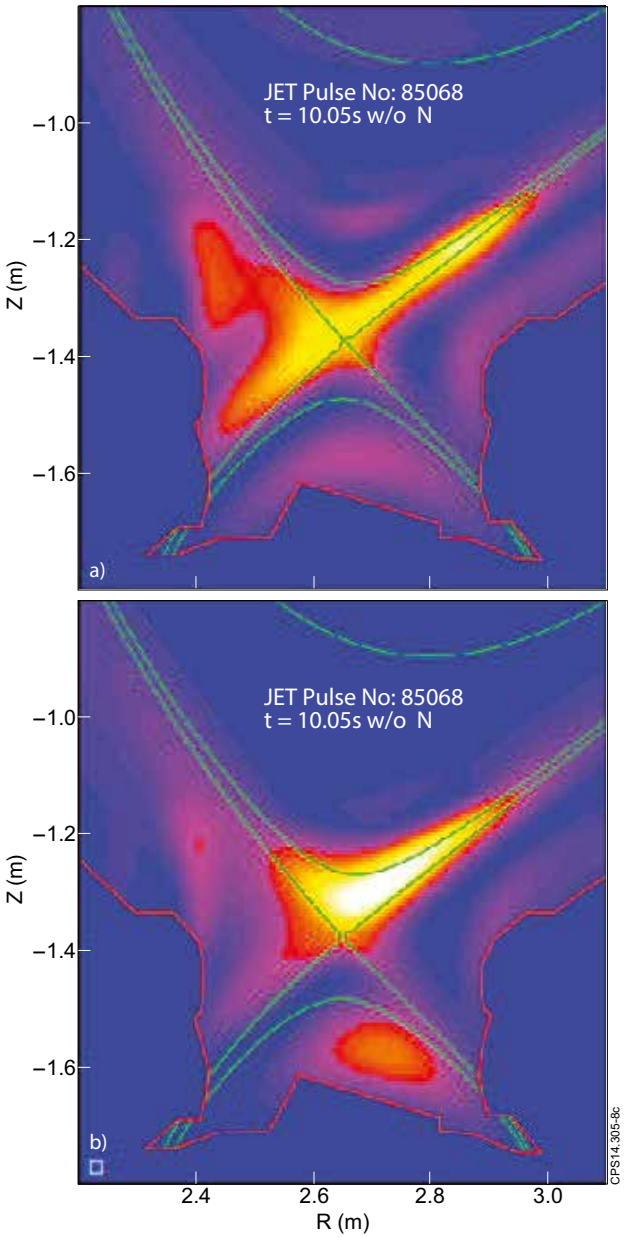

Figure 8: Total radiation distribution in the JET divertor without (a) and with (b) strong N_2 injection.

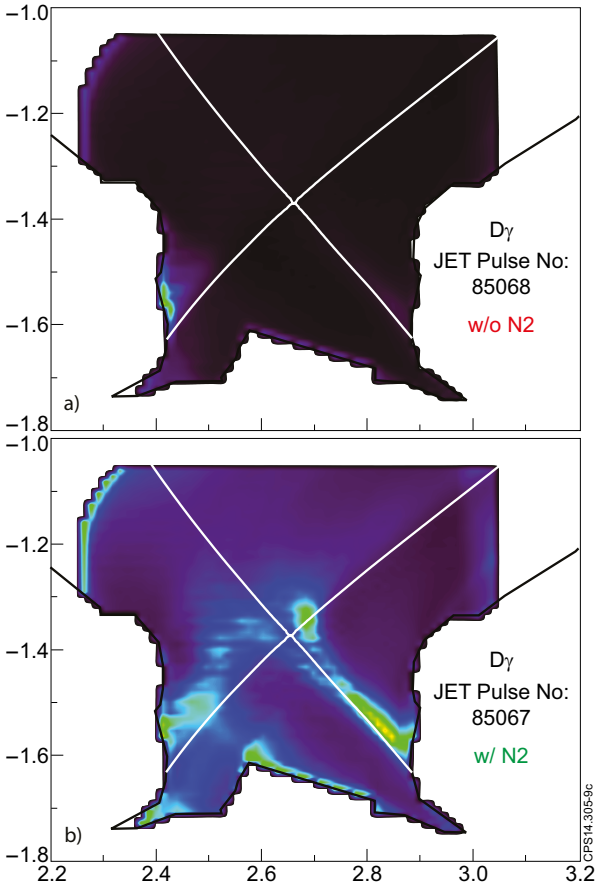

Figure 9: Dγ emission distribution in the JET divertor without (a) and with (b) strong N_2 injection.